Article

Three-Dimensional Nonlinear Optical Chromophores Based on Metal-to-Ligand Charge-Transfer from Ruthenium(II) or Iron(II) Centers

Benjamin J. Coe, James A. Harris, Bruce S. Brunschwig,
Inge Asselberghs, Koen Clays, Javier Garn, and Jess Orduna

J. Am. Chem. Soc., **2005**, 127 (38), 13399-13410• DOI: 10.1021/ja053879x • Publication Date (Web): 30 August 2005

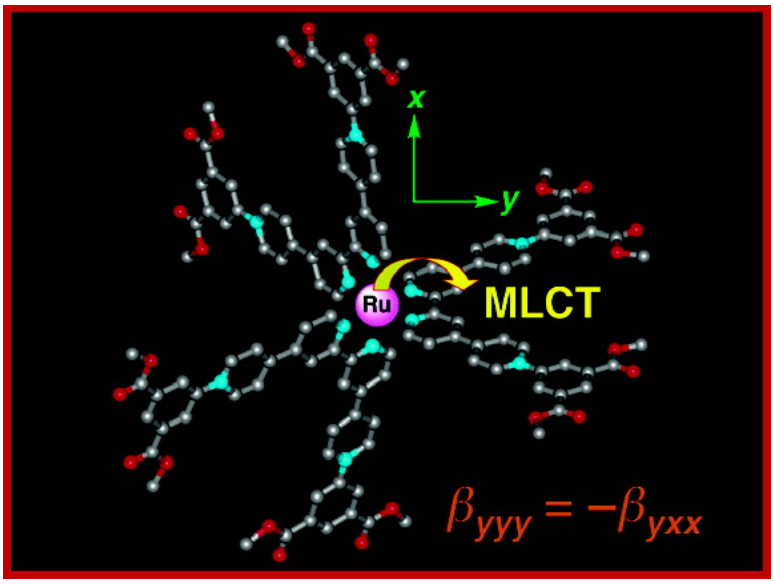

More About This Article

Additional resources and features associated with this article are available within the HTML version:

- Supporting Information
- Links to the 9 articles that cite this article, as of the time of this article download
- Access to high resolution figures
- Links to articles and content related to this article
- Copyright permission to reproduce figures and/or text from this article

View the Full Text HTML

Journal of the American Chemical Society is published by the American Chemical Society. 1155 Sixteenth Street N.W., Washington, DC 20036

J|A|C|S
ARTICLES
Published on Web 08/30/2005

Three-Dimensional Nonlinear Optical Chromophores Based on Metal-to-Ligand Charge-Transfer from Ruthenium(II) or Iron(II) Centers

Benjamin J. Coe,*[,†] James A. Harris,[†,⊥] Bruce S. Brunschwig,[‡] Inge Asselberghs,[§] Koen Clays,[§] Javier Garín,[||] and Jesús Orduna[||]

Contribution from the School of Chemistry, University of Manchester, Oxford Road, Manchester, U.K. M13 9PL, Molecular Materials Research Center, Beckman Institute, MC 139-74, California Institute of Technology, 1200 East California Boulevard, Pasadena, California 91125, Department of Chemistry, University of Leuven, Celestijnenlaan 200D, B-3001 Leuven, Belgium, and Departamento de Química Orgánica, ICMA, Universidad de Zaragoza-CSIC, E-50009 Zaragoza, Spain

Received June 13, 2005; E-mail: b.coe@man.ac.uk

Abstract: In this article, we describe a series of new complex salts in which electron-rich transition-metal centers are coordinated to three electron-accepting *N*-methyl/aryl-2,2′:4,4″:4′,4‴-quaterpyridinium ligands. These complexes contain either Ru^{II} or Fe^{II} ions and have been characterized by using various techniques, including electronic absorption spectroscopy and cyclic voltammetry. Molecular quadratic nonlinear optical (NLO) responses β have been determined by using hyper-Rayleigh scattering at 800 nm and also via Stark (electroabsorption) spectroscopic studies on the intense, visible $d \rightarrow \pi^*$ metal-to-ligand charge-transfer bands. The latter experiments reveal that these putatively octupolar D_3 chromophores exhibit two substantial components of the β tensor which are associated with transitions to dipolar excited states. Computations involving time-dependent density-functional theory and the finite field method serve to further illuminate the electronic structures and associated linear and NLO properties of the new chromophoric salts.

Introduction

Molecular nonlinear optical (NLO) materials continue to attract considerable interest on account of the promise they hold for applications in emerging optoelectronic and all-optical data processing technologies.[1] Although the majority of NLO chromophores feature relatively simple dipolar electronic structures, octupolar compounds form an increasingly important class of materials for potential quadratic (second-order) NLO applications.[2] Despite having zero net ground-state dipole moments, octupolar molecules can display large values of the first hyperpolarizability β which governs quadratic NLO effects at the molecular level. Transition-metal coordination and organometallic complexes are an interesting subclass of molecular NLO compounds which offer extensive scope for the creation of multifunctional optical materials,[3] featuring, for example, redox-switchable NLO responses.[4] Because intramolecular charge-transfer (ICT) resonances can have pronounced enhancing effects on experimentally measured β values, it is necessary to derive static first hyperpolarizabilities β_0 for comparisons between different chromophores. The often large β_0 values of metal complexes are most commonly associated with metal-to-ligand charge-transfer (MLCT) transitions.

Attention was originally drawn to the octupolar nature of D_3 tris-chelate transition-metal complexes by Zyss et al. who used hyper-Rayleigh scattering (HRS) measurements and a three-state model to obtain β_0 values of 53×10^{-30} and 47×10^{-30} esu for the salts $[Ru^{II}(bpy)_3]Br_2$ (bpy = 2,2′-bipyridyl) and $[Ru^{II}(phen)_3]Cl_2$ (phen = 1,10-phenanthroline), respectively.[5] Sub-

† University of Manchester.
‡ California Institute of Technology.
§ University of Leuven.
|| Universidad de Zaragoza.
⊥ Present address: Molecular Materials Research Center, Beckman Institute, MC 139-74, California Institute of Technology, 1200 East California Blvd., Pasadena, CA 91125.

(1) (a) Zyss, J. *Molecular Nonlinear Optics: Materials, Physics and Devices*; Academic Press: Boston, 1994. (b) Bosshard, Ch., Sutter, K., Prêtre, Ph., Hulliger, J., Flörsheimer, M., Kaatz, P., Günter, P. *Organic Nonlinear Optical Materials (Advances in Nonlinear Optics, Vol. 1)*; Gordon & Breach: Amsterdam, The Netherlands, 1995. (c) *Nonlinear Optics of Organic Molecules and Polymers*; Nalwa, H. S., Miyata, S., Eds.; CRC Press: Boca Raton, FL, 1997. (d) *Nonlinear Optical Properties of Matter: From Molecules to Condensed Phases*; Papadopoulos, M. G., Leszczynski, J., Sadlej, A. J., Eds.; Kluwer: Dordrecht, The Netherlands, 2005.

(2) Selected examples: (a) Ledoux, I.; Zyss, J.; Siegel, J. S.; Brienne J.; Lehn, J.-M. *Chem. Phys. Lett.* **1990**, *172*, 440−444. (b) Joffre, M.; Yaron, D.; Silbey, R. J.; Zyss, J. *J. Chem. Phys.* **1992**, *97*, 5607−5615. (c) Verbiest, T.; Clays, K.; Persoons, A.; Meyers, F.; Brédas, J. L. *Opt. Lett.* **1993**, *18*, 525−527. (d) Zyss, J. *J. Chem. Phys.* **1993**, *98*, 6583−6599. (e) Verbiest, T.; Clays, K.; Samyn, C.; Wolff, J.; Reinhoudt, D.; Persoons, A. *J. Am. Chem. Soc.* **1994**, *116*, 9320−9323. (f) Zyss J.; Ledoux, I. *Chem. Rev.* **1994**, *94*, 77−105. (g) Wolff, J. J.; Wortmann, R. *Adv. Phys. Org. Chem.* **1999**, *32*, 121−217. (h) Wolff, J. J.; Siegler, F.; Matschiner, R.; Wortmann, R. *Angew. Chem., Int. Ed.* **2000**, *39*, 1436−1439. (i) Cho, B. R.; Piao, M. J.; Son, K. H.; Lee, S. H.; Yoon, S. J.; Jeon, S.-J.; Cho, M.-H. *Chem.−Eur. J.* **2002**, *8*, 3907−3916. (j) Brunel, J.; Mongin, O.; Jutand, A.; Ledoux, I.; Zyss, J.; Blanchard-Desce, M. *Chem. Mater.* **2003**, *15*, 4139−4148. (k) Cui, Y. Z.; Fang, Q.; Lei, H.; Xue, G.; Yu, W. T. *Chem. Phys. Lett.* **2003**, *377*, 507−511. (l) Ray, P. C.; Leszczynski, J. *Chem. Phys. Lett.* **2004**, *399*, 162−166. (m) Claessens, C. G.; González-Rodríguez, D.; Torres, T.; Martín, G.; Agulló-Lopez, F.; Ledoux, I.; Zyss, J.; Ferro, V. R.; García de la Vega, J. M. *J. Phys. Chem. B* **2005**, *109*, 3800−3806. (n) Le Floc'h, V.; Brasselet, S.; Zyss, J.; Cho, B. R.; Lee, S. H.; Jeon, S.-J.; Cho, M.-H.; Min, K. S.; Suh, M. P. *Adv. Mater.* **2005**, *17*, 196−200.

sequent HRS studies afforded a huge β_0 of 2200×10^{-30} for a $[Ru^{II}(bpy)_3]^{2+}$ derivative bearing electron-donating styryl substituents.[6] However, it has been found that this β_0 value is overestimated due to contributions from two-photon luminescence,[7] and more recent studies have accordingly given a smaller (although still large) β_0 of 380×10^{-30} esu for this complex.[8] A number of other NLO studies have recently been carried out with derivatives of $[Ru^{II}(bpy)_3]^{2+}$ and related complexes of other metals.[8,9] Although the basic $[Ru^{II}(bpy)_3]^{2+}$ and related complex units themselves have octupolar ground states, polarized HRS and Stark spectroscopic measurements have shown that the β responses of their derivatives are better described as arising from multiple degenerate dipolar ICT transitions, rather than an octupolar transition.[10] Furthermore, the dominant transitions correspond with intraligand charge-transfer (ILCT) excitations which are red-shifted on metal coordination and are directionally opposed to the MLCT transitions.[8,10] Since all previous NLO studies with such tris-chelate complexes have involved ligands with electron-donating groups,[6,8,9] we reasoned that it would be interesting to prepare related species in which the ligands are substituted with electron-withdrawing pyridinium groups. In contrast with previously studied chromophores, the simpler electronic structures of our new complexes mean that only MLCT transitions determine their NLO properties, introducing greater scope for rational maximization and metal-based redox-switching of β_0 responses.

Experimental Section

Materials and Procedures. All reactions were performed under an Ar atmosphere and in Ar-purged solvents. The compounds *cis*-$Ru^{II}Cl_2(DMSO)_4$,[11] 2,2′:4,4″:4′,4‴-quaterpyridyl (Qpy),[12] *N*″,*N*‴-dimethyl-2,2′:4,4″:4′,4‴-quaterpyridinium hexafluorophosphate ($[Me_2Qpy^{2+}][PF_6]_2$),[13] *N*″,*N*‴-diphenyl-2,2′:4,4″:4′,4‴-quaterpyridinium hexafluorophosphate ($[Ph_2Qpy^{2+}][PF_6]_2$),[12] and *N*″,*N*‴-di(4-acetylphenyl)-2,2′:4,4″:4′,4‴-quaterpyridinium hexafluorophosphate ($[(4\text{-}AcPh)_2Qpy^{2+}][PF_6]_2$)[12] were prepared according to published procedures. All other reagents were obtained commercially and used as supplied. Products were dried overnight in a vacuum desiccator ($CaSO_4$) prior to characterization.

General Physical Measurements. ^{1}H NMR spectra were recorded on a Varian Gemini 200 spectrometer, and all shifts are referenced to TMS. The fine splitting of pyridyl or phenyl ring AA′BB′ patterns is ignored, and the signals are reported as simple doublets, with *J* values referring to the two most intense peaks. Elemental analyses were performed by the Microanalytical Laboratory, University of Manchester, and UV−visible spectra were obtained by using a Hewlett-Packard 8452A diode array spectrophotometer.

Cyclic voltammetric measurements were carried out by using an EG&G PAR model 283 potentiostat/galvanostat. A single-compartment cell was used with a silver/silver chloride reference electrode separated by a salt bridge from a Pt or a glassy carbon disk working electrode and Pt wire auxiliary electrode. Acetonitrile was freshly distilled (from CaH_2), and $[NBu^n_4]PF_6$, twice recrystallized from ethanol and dried in vacuo, was used as the supporting electrolyte. Solutions containing ca. 10^{-3} M analyte (0.1 M electrolyte) were deaerated by purging with N_2. All $E_{1/2}$ values were calculated from $(E_{pa} + E_{pc})/2$ at a scan rate of 200 mV s^{-1}.

Synthesis of *N*″,*N*‴-Di(2,4-dinitrophenyl)-2,2′:4,4″:4′,4‴-quaterpyridinium Hexafluorophosphate, $[(2,4\text{-}DNPh)_2Qpy^{2+}][PF_6]_2$. A mixture of Qpy·$0.5H_2O$ (1.0 g, 3.13 mmol) and 2,4-dinitrochlorobenzene (6.34 g, 31.3 mmol) in ethanol (60 mL) was heated at reflux for 72 h. Addition of $CHCl_3$ produced a white precipitate which was filtered off, washed with diethyl ether, and dried to yield crude *N*″,*N*‴-di(2,4-dinitrophenyl)-2,2′:4,4″:4′,4‴-quaterpyridinium chloride ($[(2,4\text{-}DNPh)_2Qpy^{2+}]Cl_2$). This solid was dissolved in water, and addition of aqueous NH_4PF_6 resulted in a white precipitate which was filtered off, washed with water, and dried. Further purification was effected by precipitation from acetone/diethyl ether: 534 mg, 18%; δ_H (CD_3COCD_3) 9.68 (4 H, d, $J = 7.0$ Hz, C_5H_4N), 9.32 (2 H, d, $J = 2.4$ Hz, C_6H_3), 9.21 (2 H, d, $J = 1.1$ Hz, C_5H_3N), 9.15−9.06 (8 H, m, C_5H_4N, C_6H_3, C_5H_3N), 8.66 (2 H, d, $J = 8.7$ Hz, C_6H_3), 8.31 (2 H, dd, $J = 5.1$, 1.9 Hz, C_5H_3N). Anal. Calcd (%) for $C_{32}H_{20}F_{12}N_8O_8P_2$: C, 41.13; H, 2.16; N, 11.99. Found: C, 41.27; H, 2.02; N, 11.67.

Synthesis of *N*″,*N*‴-Di(3,5-bismethoxycarbonylphenyl)-2,2′:4,4″:4′,4‴-quaterpyridinium Hexafluorophosphate, $[(3,5\text{-}MCPh)_2Qpy^{2+}][PF_6]_2$. A mixture of Qpy·$0.5H_2O$ (500 mg, 1.57 mmol) and 2,4-dinitrochlorobenzene (3.18 g, 15.7 mmol) in ethanol (40 mL) was heated at reflux for 72 h. Addition of $CHCl_3$ produced a white precipitate which was filtered off, washed with diethyl ether, and dried to yield crude *N*″,*N*‴-di(2,4-dinitrophenyl)-2,2′:4,4″:4′,4‴-quaterpyridinium chloride ($[(2,4\text{-}DNPh)_2Qpy^{2+}]Cl_2$). This solid was suspended in ethanol (50 mL) with dimethoxy-5-aminoisophthalate (3.27 g, 15.6 mmol) and

(3) (a) Nalwa, H. S. *Appl. Organomet. Chem.* **1991**, *5*, 349−377. (b) Marder, S. R. In *Inorganic Materials*, 2nd ed.; Bruce, D. W., O'Hare, D., Eds.; Wiley: Chichester, U.K., 1992; pp 121−169. (c) Kanis, D. R.; Ratner, M. A.; Marks, T. J. *Chem. Rev.* **1994**, *94*, 195−242. (d) Long, N. J. *Angew. Chem., Int. Ed. Engl.* **1995**, *34*, 21−38. (e) Whittall, I. R.; McDonagh, A. M.; Humphrey, M. G.; Samoc, M. *Adv. Organomet. Chem.* **1998**, *42*, 291−362. (f) Whittall, I. R.; McDonagh, A. M.; Humphrey, M. G.; Samoc, M. *Adv. Organomet. Chem.* **1998**, *43*, 349−405. (g) Heck, J.; Dabek, S.; Meyer-Friedrichsen, T.; Wong, H. *Coord. Chem. Rev.* **1999**, *190−192*, 1217−1254. (h) Gray, G. M.; Lawson, C. M. In *Optoelectronic Properties of Inorganic Compounds*; Roundhill, D. M., Fackler, J. P., Jr., Eds.; Plenum: New York, 1999; pp 1−27. (i) Shi, S. In *Optoelectronic Properties of Inorganic Compounds*; Roundhill, D. M., Fackler, J. P., Jr., Eds.; Plenum: New York, 1999; pp 55−105. (j) Le Bozec, H.; Renouard, T. *Eur. J. Inorg. Chem.* **2000**, 229−239. (k) Barlow, S.; Marder, S. R. *Chem. Commun.* **2000**, 1555−1562. (l) Lacroix, P. G. *Eur. J. Inorg. Chem.* **2001**, 339−348. (m) Di Bella, S. *Chem. Soc. Rev.* **2001**, *30*, 355−366. (n) Coe, B. J. In *Comprehensive Coordination Chemistry II*; McCleverty J. A., Meyer, T. J., Eds.; Elsevier Pergamon: Oxford, U.K., 2004; Vol. 9, pp 621−687.

(4) (a) Coe, B. J.; Houbrechts, S.; Asselberghs, I.; Persoons, A. *Angew. Chem., Int. Ed.* **1999**, *38*, 366−369. (b) Coe, B. J. *Chem.−Eur. J.* **1999**, *5*, 2464−2471. (c) Weyland, T.; Ledoux, I.; Brasselet, S.; Zyss, J.; Lapinte, C. *Organometallics* **2000**, *19*, 5235−5237. (d) Malaun, M.; Reeves, Z. R.; Paul, R. L.; Jeffery, J. C.; McCleverty, J. A.; Ward, M. D.; Asselberghs, I.; Clays, K.; Persoons, A. *Chem. Commun.* **2001**, 49−50. (e) Malaun, M. et al. *J. Chem. Soc., Dalton Trans.* **2001**, 3025−3038. (f) Cifuentes, M. P.; Powell, C. E.; Humphrey, M. G.; Heath, G. A.; Samoc, M.; Luther-Davies B. *J. Phys. Chem. A* **2001**, *105*, 9625−9627. (g) Paul, F.; Costuas, K.; Ledoux, I.; Deveau, S.; Zyss, J.; Halet, J.-F.; Lapinte, C. *Organometallics* **2002**, *21*, 5229−5235. (h) Powell, C. E.; Cifuentes, M. P.; Morrall, J. P.; Stranger, R.; Humphrey, M. G.; Samoc, M.; Luther-Davies, B.; Heath, G. A. *J. Am. Chem. Soc.* **2003**, *125*, 602−610. (i) Asselberghs, I.; Clays, K.; Persoons, A.; McDonagh, A. M.; Ward, M. D.; McCleverty, J. A. *Chem. Phys. Lett.* **2003**, *368*, 408−411. (j) Powell, C. E.; Humphrey, M. G.; Cifuentes, M. P.; Morrall, J. P.; Samoc, M.; Luther-Davies, B. *J. Phys. Chem. A* **2003**, *107*, 11264−11266. (k) Sporer, C. et al. *Angew. Chem., Int. Ed.* **2004**, *43*, 5266−5268.

(5) Zyss, J.; Dhenaut, C.; Chauvan, T.; Ledoux, I. *Chem. Phys. Lett.* **1993**, *206*, 409−414.

(6) Dhenaut, C.; Ledoux, I.; Samuel, I. D. W.; Zyss, J.; Bourgault, M.; Le Bozec, H. *Nature* **1995**, *374*, 339−342.

(7) Morrison, I. D.; Denning, R. G.; Laidlaw, W. M.; Stammers, M. A. *Rev. Sci. Instrum.* **1996**, *67*, 1445−1453.

(8) Le Bozec, H.; Renouard, T.; Bourgault, M.; Dhenaut, C.; Brasselet, S.; Ledoux, I.; Zyss, J. *Synth. Met.* **2001**, *124*, 185−189.

(9) Selected examples: (a) Le Bouder, T.; Maury, O.; Le Bozec, H.; Ledoux, I.; Zyss, J. *Chem. Commun.* **2001**, 2430−2431. (b) Le Bozec, H.; Le Bouder, T.; Maury, O.; Bondon, A.; Ledoux, I.; Deveau, S.; Zyss, J. *Adv. Mater.* **2001**, *13*, 1677−1681. (c) Sénéchal, K.; Maury, O.; Le Bozec, H.; Ledoux, I.; Zyss, J. *J. Am. Chem. Soc.* **2002**, *124*, 4560−4561. (d) Le Bouder, T.; Maury, O.; Bondon, O.; Costuas, K.; Amouyal, E.; Ledoux, I.; Zyss, J.; Le Bozec, H. *J. Am. Chem. Soc.* **2003**, *125*, 12284−12299. (e) Viau, L.; Bidault, S.; Maury, O.; Brasselet, S.; Ledoux, I.; Zyss, J.; Ishow, E.; Nakatani, K.; Le Bozec, H. *J. Am. Chem. Soc.* **2004**, *126*, 8386−8387. (f) Maury, O.; Viau, L.; Sénéchal, K.; Corre, B.; Guégan, J.-P.; Renouard, T.; Ledoux, I.; Zyss, J.; Le Bozec, H. *Chem.−Eur. J.* **2004**, *10*, 4454−4466.

(10) Vance, F. W.; Hupp, J. T. *J. Am. Chem. Soc.* **1999**, *121*, 4047−4053.

(11) Evans, I. P.; Spencer, A.; Wilkinson, G. *J. Chem. Soc., Dalton Trans.* **1973**, 204−209.

(12) Coe, B. J.; Harris, J. A.; Jones, L. A.; Brunschwig, B. S.; Song, K.; Clays, K.; Garín, J.; Orduna, J.; Coles, S. J.; Hursthouse, M. B. *J. Am. Chem. Soc.* **2005**, *127*, 4845−4859.

(13) Morgan, R. J.; Baker, A. D. *J. Org. Chem.* **1990**, *55*, 1986−1993.

heated at reflux for 50 h. The resulting solution was reduced to dryness and the solid washed with acetone under filtration. The remaining solid was dissolved in water and extracted with $CHCl_3$ (2 × 200 mL). Addition of aqueous NH_4PF_6 to the aqueous layer produced a gray/blue precipitate which was filtered off, washed with water, and dried. Further purification was afforded by precipitation from acetone/diethyl ether: 492 mg, 31%; δ_H (CD_3COCD_3) 9.75 (4 H, d, J = 7.0 Hz, C_5H_4N), 9.18 (2 H, d, J = 1.1 Hz, C_5H_3N), 9.13 (2 H, d, J = 5.4 Hz, C_5H_3N), 9.08 (4 H, d, J = 7.0 Hz, C_5H_4N), 8.89 (2 H, d, J = 1.3 Hz, C_6H_3), 8.87 (4 H, d, J = 1.4 Hz, C_6H_3), 8.28 (2 H, dd, J = 4.8, 1.6 Hz, C_5H_3N), 4.03 (12 H, s, Me). Anal. Calcd (%) for $C_{40}H_{32}F_{12}N_4O_8P_2$·0.5$H_2O$: C, 48.25; H, 3.34; N, 5.63. Found: C, 48.24; H, 3.34; N, 5.63.

Synthesis of $[Ru^{II}(Me_2Qpy^{2+})_3][PF_6]_8$ 1. A mixture of *cis*-$Ru^{II}Cl_2(DMSO)_4$ (33 mg, 0.068 mmol), silver(I) tosylate ($AgC_7H_7SO_3$, 38 mg, 0.136 mmol), and $[Me_2Qpy^{2+}][PF_6]_2$ (150 mg, 0.238 mmol) in degassed DMF (10 mL) was heated at reflux for 3 h under Ar. The resulting orange/brown solution was cooled to room temperature, and the AgCl precipitate was filtered off. Addition of diethyl ether to the filtrate afforded a brown precipitate which was filtered off and then dissolved in water. Addition of aqueous NH_4PF_6 to the filtrate produced an orange/red precipitate which was filtered off, washed with water, and dried. The crude product was dissolved in acetone, and addition of a solution of $[NBu^n_4]Cl$ in acetone afforded a brown precipitate. This solid was filtered off, washed with acetone, and dissolved in water (5 mL). Careful addition of acetone (60 mL) resulted in a fine brown precipitate which was filtered off, washed with acetone, and then dissolved in water. Addition of aqueous NH_4PF_6 produced an orange/red precipitate which was filtered off, washed with water, and dried. An acetone solution of the crude product was loaded onto a silica gel column (230−400 mesh, 5 × 22 cm) and eluted with 0.1 M NH_4PF_6 in acetonitrile. Fractions were collected and compared by TLC. Similar fractions were combined, reduced to dryness, and precipitated from acetone/aqueous NH_4PF_6. Further purification was achieved by reprecipitations from acetone/ethanol and finally from acetone/dichloromethane to afford an orange/red solid: 55 mg, 35%; δ_H (CD_3COCD_3) 9.51 (6 H, d, J = 1.3 Hz, C_5H_3N), 9.24 (12 H, d, J = 7.0 Hz, C_5H_4N), 8.66 (12 H, d, J = 6.9 Hz, C_5H_4N), 8.47 (6 H, d, J = 5.9 Hz, C_5H_3N), 8.11 (6 H, dd, J = 5.9, 1.7 Hz, C_5H_3N), 4.71 (18 H, s, Me). Anal. Calcd (%) for $C_{66}H_{60}F_{48}N_{12}P_8Ru$·3$H_2O$: C, 33.93; H, 2.85; N, 7.19. Found: C, 33.85; H, 2.74; N, 7.03.

Synthesis of $[Ru^{II}(Ph_2Qpy^{2+})_3][PF_6]_8$ 2. This compound was prepared and purified in a manner similar to **1** by using $[Ph_2Qpy^{2+}][PF_6]_2$ (180 mg, 0.239 mmol) instead of $[Me_2Qpy^{2+}][PF_6]_2$. The column was eluted with 0.1 M NH_4PF_6 in 5:1 methanol−acetone to afford a red solid: 101 mg, 54%; δ_H (CD_3COCD_3) 9.64 (6 H, d, J = 1.6 Hz, C_5H_3N), 9.59 (12 H, d, J = 7.0 Hz, C_5H_4N), 8.85 (12 H, d, J = 7.0 Hz, C_5H_4N), 8.57 (6 H, d, J = 6.1 Hz, C_5H_3N), 8.22 (6 H, dd, J = 6.0, 1.8 Hz, C_5H_3N), 8.05−8.00 (12 H, m, Ph), 7.98−7.81 (18 H, m, Ph). Anal. Calcd (%) for $C_{96}H_{72}F_{48}N_{12}P_8Ru$·4$H_2O$: C, 42.29; H, 2.96; N, 6.16. Found: C, 42.18; H, 2.82; N, 6.13.

Synthesis of $[Ru^{II}\{(4\text{-}AcPh)_2Qpy^{2+}\}_3][PF_6]_8$ 3. This compound was prepared and purified in an identical manner to **2** by using $[(4\text{-}AcPh)_2Qpy^{2+}][PF_6]_2$·1.5$H_2O$ (207 mg, 0.239 mmol) instead of $[Ph_2Qpy^{2+}][PF_6]_2$ to afford a dark red solid: 48 mg, 23%; δ_H (CD_3COCD_3) 9.66−9.64 (18 H, m, C_5H_3N + C_5H_4N), 8.88 (12 H, d, J = 6.7 Hz, C_5H_4N), 8.57 (6 H, d, J = 6.0 Hz, C_5H_3N), 8.39 (12 H, d, J = 8.5 Hz, C_6H_4), 8.21−8.17 (18 H, m, C_5H_3N + C_6H_4), 2.74 (18 H, s, Me). Anal. Calcd (%) for $C_{108}H_{84}F_{48}N_{12}O_6P_8Ru$·6$H_2O$: C, 43.03; H, 3.21; N, 5.58. Found: C, 42.93; H, 2.94; N, 5.62.

Synthesis of $[Ru^{II}\{(3,5\text{-}MCPh)_2Qpy^{2+}\}_3][PF_6]_8$ 4. This compound was prepared and purified in an identical manner to **1** by using $[(3,5\text{-}MCPh)_2Qpy^{2+}][PF_6]_2$·0.5$H_2O$ (237 mg, 0.238 mmol) instead of $[Me_2Qpy^{2+}][PF_6]_2$ to afford a dark red solid: 112 mg, 47%; δ_H (CD_3COCD_3) 9.74 (12 H, d, J = 7.0 Hz, C_5H_4N), 9.65 (6 H, d, J = 1.1 Hz, C_5H_3N), 8.93 (12 H, d, J = 7.0 Hz, C_5H_4N), 8.87 (6 H, d, J = 1.3 Hz, C_6H_3), 8.84 (12 H, d, J = 1.3 Hz, C_6H_3), 8.59 (6 H, d, J = 6.1 Hz, C_5H_3N), 8.25 (6 H, dd, J = 5.7, 1.3 Hz, C_5H_3N), 4.01 (36 H, s, Me). Anal. Calcd (%) for $C_{120}H_{96}F_{48}N_{12}O_{24}P_8Ru$·7$H_2O$: C, 41.45; H, 3.19; N, 4.83. Found: C, 41.36; H, 2.74; N, 4.78.

Synthesis of $[Fe^{II}(Me_2Qpy^{2+})_3][PF_6]_8$ 5. A mixture of $Fe^{II}(BF_4)_2$·6H_2O (32 mg, 0.095 mmol) and $[Me_2Qpy^{2+}][PF_6]_2$ (209 mg, 0.332 mmol) in degassed acetone was heated at reflux for 4 h. After cooling to room temperature, the reaction solution was filtered, and addition of a solution of $[NBu^n_4]Cl$ in acetone afforded a dark solid which was filtered off, washed with acetone, and dissolved in water (5 mL). Careful addition of acetone (50 mL) afforded a fine red/purple precipitate which was filtered off, washed with acetone, and then dissolved in water. Addition of aqueous NH_4PF_6 produced an orange/red precipitate which was filtered off, washed with water, and dried. An acetone solution of the crude product was loaded onto a silica gel column (230−400 mesh, 5 × 22 cm) and eluted with 0.1 M NH_4PF_6 in 10:1 acetonitrile−toluene. Fractions were collected and compared by TLC. Similar fractions were combined, reduced to dryness, and precipitated from acetone/aqueous NH_4PF_6. Further purification was achieved by precipitations from acetone/ethanol to afford an orange/red solid: 73 mg, 34%; δ_H (CD_3COCD_3) 9.53 (6 H, s, C_5H_3N), 9.26 (12 H, d, J = 6.2 Hz, C_5H_4N), 8.66 (12 H, d, J = 6.2 Hz, C_5H_4N), 8.16 (6 H, d, J = 5.9 Hz, C_5H_3N), 8.10 (6 H, d, J = 6.2 Hz, C_5H_3N), 4.71 (18 H, s, Me). Anal. Calcd (%) for $C_{66}H_{60}F_{48}N_{12}P_8Fe$·3$H_2O$: C, 34.60; H, 2.90; N, 7.34. Found: C, 34.46; H, 2.70; N, 7.23.

Synthesis of $[Fe^{II}(Ph_2Qpy^{2+})_3][PF_6]_8$ 6. This compound was prepared in an identical manner to **5** by using $Fe^{II}(BF_4)_2$·6H_2O (28 mg, 0.083 mmol) and $[Ph_2Qpy^{2+}][PF_6]_2$ (221 mg, 0.293 mmol) instead of $[Me_2Qpy^{2+}][PF_6]_2$. The product was purified by using preparative scale chromatography on a silica plate, eluting with 0.1 M NH_4PF_6 in 4:1 methanol−acetonitrile. Further purification was achieved by precipitations from acetone/aqueous NH_4PF_6 to afford a black solid: 40 mg, 18%; δ_H (CD_3COCD_3) 9.67 (6 H, s, C_5H_3N), 9.60 (12 H, d, J = 7.0 Hz, C_5H_4N), 8.85 (12 H, d, J = 7.0 Hz, C_5H_4N), 8.26 (6 H, d, J = 5.9 Hz, C_5H_3N), 8.22 (6 H, d, J = 6.1 Hz, C_5H_3N), 8.05−8.00 (12 H, m, Ph), 7.85−7.81 (18 H, m, Ph). Anal. Calcd (%) for $C_{96}H_{72}F_{48}N_{12}P_8Fe$·4$H_2O$: C, 43.00; H, 3.01; N, 6.27. Found: C, 42.99; H, 2.69; N, 6.15.

Synthesis of $[Fe^{II}\{(4\text{-}AcPh)_2Qpy^{2+}\}_3][PF_6]_8$ 7. This compound was prepared and purified in a manner similar to **5** using of $Fe^{II}(BF_4)_2$·6H_2O (31 mg, 0.092 mmol) and $[(4\text{-}AcPh)_2Qpy^{2+}][PF_6]_2$·1.5$H_2O$ (279 mg, 0.322 mmol) instead of $[Me_2Qpy^{2+}][PF_6]_2$. The column was eluted with 0.1 M NH_4PF_6 in 3:1 toluene−acetonitrile to afford a black solid: 130 mg, 49%; δ_H (CD_3COCD_3) 9.68−9.64 (18 H, m, C_5H_3N + C_5H_4N), 8.87 (12 H, d, J = 7.0 Hz, C_5H_4N), 8.39 (12 H, d, J = 8.8 Hz, C_6H_4), 8.28−8.16 (24 H, m, C_5H_3N + C_6H_4), 2.73 (18 H, s, Me). Anal. Calcd (%) for $C_{108}H_{84}F_{48}N_{12}O_6P_8Fe$·2$H_2O$: C, 44.77; H, 3.06; N, 5.80. Found: C, 44.60; H, 2.85; N, 5.81.

Hyper-Rayleigh Scattering. General details of the hyper-Rayleigh scattering (HRS) experiment have been discussed elsewhere,[14] and the experimental procedure used was as previously described.[15,16] Measurements were carried out in acetonitrile, with the octupolar crystal violet as an external reference ($\beta_{yyy,800}$ = 500 × 10^{-30} esu in acetonitrile, from the value of 340 × 10^{-30} esu in methanol,[16] corrected for local field factors at optical frequencies). All measurements were performed by using the 800 nm fundamental of a regenerative mode-locked Ti^{3+}:sapphire laser (Spectra Physics, model Tsunami, 100 fs pulses, 1 W, 80 MHz). Samples were filtered (Millipore, 0.45 μm), and dilute

(14) (a) Terhune, R. W.; Maker, P. D.; Savage, C. M. *Phys. Rev. Lett.* **1965**, *14*, 681−684. (b) Clays, K.; Persoons, A. *Phys. Rev. Lett.* **1991**, *66*, 2980−2983. (c) Clays, K.; Persoons, A. *Rev. Sci. Instrum.* **1992**, *63*, 3285−3289. (d) Hendrickx, E.; Clays, K.; Persoons, A. *Acc. Chem. Res.* **1998**, *31*, 675−683.

(15) Clays, K.; Olbrechts, G.; Munters, T.; Persoons, A.; Kim, O.-K.; Choi, L.-S. *Chem. Phys. Lett.* **1998**, *293*, 337−342.

(16) Olbrechts, G.; Strobbe, R.; Clays, K.; Persoons, A. *Rev. Sci. Instrum.* **1998**, *69*, 2233−2241.

solutions ($10^{-5}-10^{-6}$ M) were used to ensure a linear dependence of $I_{2\omega}/I_{\omega}^{2}$ on solute concentration, precluding the need for Lambert−Beer correction factors. A relative error of ±15% is estimated for the β values derived from these measurements.

Stark Spectroscopy. The Stark apparatus, experimental methods, and data analysis procedure were exactly as previously reported,[17,18] with the only modification being that a Xe arc lamp was used as the light source in place of a W filament bulb. The Stark spectrum for each compound was measured a minimum of three times using different field strengths, and the signal was always found to be quadratic in the applied field. To fit the Stark data, the absorption spectrum was modeled with combinations of Gaussian curves that reproduce the data and separate the peaks. After taking the first and second derivatives of the model, the Liptay equation was used to yield the dipole moment change ($\Delta\mu_{12}$) associated with each of the optical transitions considered in the fit. For all of the complexes, three or four Gaussian functions were necessary to fit the absorption spectrum. In each case, two of the Gaussian curves contributed the majority of the Stark signal, so the data yielded by the insignificant components have been neglected.

The Liptay equation is:[19]

$$\Delta\epsilon(\nu)/\nu = \left[A_x\epsilon(\nu)/\nu + \frac{B_x}{15h}\frac{\partial(\epsilon(\nu)/\nu)}{\partial\nu} + \frac{C_x}{30h^2}\frac{\partial^2(\epsilon(\nu)/\nu)}{\partial\nu^2}\right]\mathbf{F}_{\text{int}}^2 \quad (1)$$

where ν is the frequency of the light in hertz, and the internal electric field is related to the applied external field by $\mathbf{F}_{\text{int}} = f_{\text{int}}\mathbf{F}_{\text{ext}}$. Butyronitrile was used as the glassing medium, for which the local field correction f_{int} is estimated as 1.33.[17,18] A two-state analysis of the MLCT transitions gives

$$\Delta\mu_{\text{ab}}^2 = \Delta\mu_{12}^2 + 4\mu_{12}^2 \quad (2)$$

where $\Delta\mu_{\text{ab}}$ is the dipole moment difference between the diabatic states, $\Delta\mu_{12}$ is the observed (adiabatic) dipole moment difference, and μ_{12} is the transition dipole moment. The latter can be determined from the oscillator strength f_{os} of the transition by

$$|\mu_{12}| = [f_{\text{os}}/(1.08 \times 10^{-5}\, E_{\text{max}})]^{1/2} \quad (3)$$

where E_{max} is the energy of the MLCT maximum (in wavenumbers). The degree of delocalization c_{b}^2 and electronic coupling matrix element H_{ab} for the diabatic states are given by

$$c_{\text{b}}^2 = \frac{1}{2}\left[1 - \left(\frac{\Delta\mu_{12}^2}{\Delta\mu_{12}^2 + 4\mu_{12}^2}\right)^{1/2}\right] \quad (4)$$

$$|H_{\text{ab}}| = \left|\frac{E_{\text{max}}(\mu_{12})}{\Delta\mu_{\text{ab}}}\right| \quad (5)$$

If the hyperpolarizability tensor β_0 has only nonzero elements along the charge-transfer direction, then this quantity is given by (perturbation series convention)[20]

$$\beta_0 = \frac{3\Delta\mu_{12}(\mu_{12})^2}{(E_{\text{max}})^2} \quad (6)$$

A relative error of ±20% is estimated for the β_0 values derived from the Stark data and using eq 6.

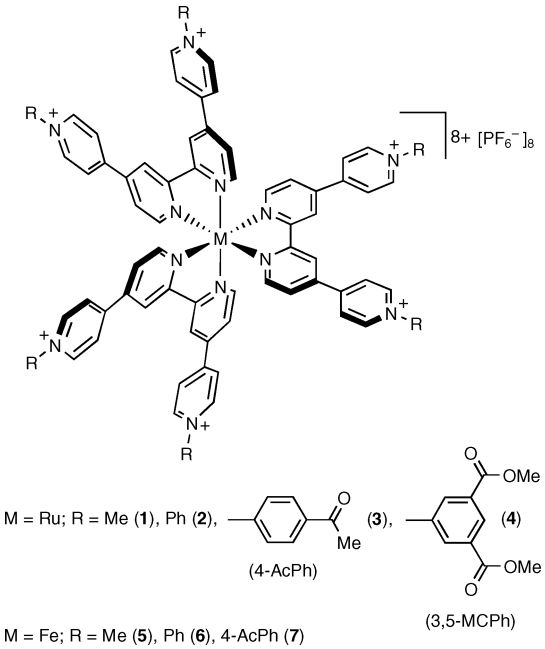

Figure 1. Chemical structures of the complex salts investigated.

Computational Procedures. All theoretical calculations were performed by using the Gaussian 03[21] program. The molecular geometries were optimized assuming D_3 symmetry by using the hybrid functional B3P86[22] and the LanL2DZ[23] basis set. The same model chemistry was used for properties calculations. Electronic transitions were calculated by means of the TD-DFT method, and the excited-state dipole moments were calculated by using the one-particle RhoCI density. The default Gaussian 03 parameters were used in every case. Molecular orbital contours were plotted by using Molekel 4.3.[24]

Results and Discussion

Synthetic Studies. The new pro-ligand salts, $[R_2Qpy^{2+}][PF_6]_2$ [R = 2,4-dinitrophenyl (2,4-DNPh) or 3,5-bismethoxycarbonylphenyl (3,5-MCPh)], were synthesized via methods which we have used to prepare analogous 4,4′-bipyridyl and Qpy-based compounds (Scheme 1).[12,25] The compound $[(2,4\text{-DNPh})_2Qpy^{2+}]Cl_2$ was used previously as a synthetic intermediate,[12] but was not purified or characterized. Complex salt **1** is a known compound, having been investigated with regard to light-induced electron-transfer reactions.[26] No synthetic details were given, but a reaction scheme indicated methylation of $[Ru^{II}(Qpy)_3]Cl_2$. In this study, complex salts **1**−**4** (Figure 1) were prepared directly by using prequaternized ligands and established coor-

(17) Coe, B. J.; Harris, J. A.; Brunschwig, B. S. *J. Phys. Chem. A* **2002**, *106*, 897−905.
(18) Shin, Y. K.; Brunschwig, B. S.; Creutz, C.; Sutin, N. *J. Phys. Chem.* **1996**, *100*, 8157−8169.
(19) (a) Liptay, W. In *Excited States*; Lim, E. C., Ed.; Academic Press: New York, 1974; Vol. 1, pp 129−229. (b) Bublitz, G. U.; Boxer, S. G. *Annu. Rev. Phys. Chem.* **1997**, *48*, 213−242.
(20) Willetts, A.; Rice, J. E.; Burland, D. M.; Shelton, D. P. *J. Chem. Phys.* **1992**, *97*, 7590−7599.
(21) Frisch, M. J. et al. *Gaussian 03*, revision B.05; Gaussian, Inc.: Pittsburgh, PA, 2003.
(22) The B3P86 functional consists of Becke's three parameter hybrid functional (Becke, A. D. *J. Chem. Phys.* **1993**, *98*, 5648−5652), with the nonlocal correlation provided by the Perdew 86 expression: Perdew, J. P. *Phys. Rev. B* **1986**, *33*, 8822−8824.
(23) D95 on first row: Dunning, T. H.; Hay, P. J. In *Modern Theoretical Chemistry*: Schaefer, H. F. III, Ed.; Plenum: New York, 1976; Vol. 3, p 1. Los Alamos ECP plus DZ on Na−Bi: (a) Hay, P. J.; Wadt, W. R. *J. Chem. Phys.* **1985**, *82*, 270−283. (b) Wadt, W. R.; Hay, P. J. *J. Chem. Phys.* **1985**, *82*, 284−298. (c) Hay, P. J.; Wadt, W. R. *J. Chem. Phys.* **1985**, *82*, 299−310.
(24) Portmann, S.; Lüthi, H. P. *Chimia* **2000**, *54*, 766−770.
(25) (a) Coe, B. J.; Harris, J. A.; Harrington, L. J.; Jeffery, J. C.; Rees, L. H.; Houbrechts, S.; Persoons, A. *Inorg. Chem.* **1998**, *37*, 3391−3399. (b) Coe, B. J.; Harris, J. A.; Asselberghs, I.; Persoons, A.; Jeffery, J. C.; Rees, L. H.; Gelbrich, T.; Hursthouse, M. B. *J. Chem. Soc., Dalton Trans.* **1999**, 3617−3625.
(26) (a) Dürr, H.; Thiery, U. *New J. Chem.* **1989**, *13*, 575−577. (b) Dürr, H.; Bossmann, S.; Schwarz, R.; Kropf, M.; Hayo, R.; Turro, N. J. *J. Photobiol. A: Chem.* **1994**, *80*, 341−350.

Scheme 1. Syntheses of the Qpy-Based Pro-Ligands

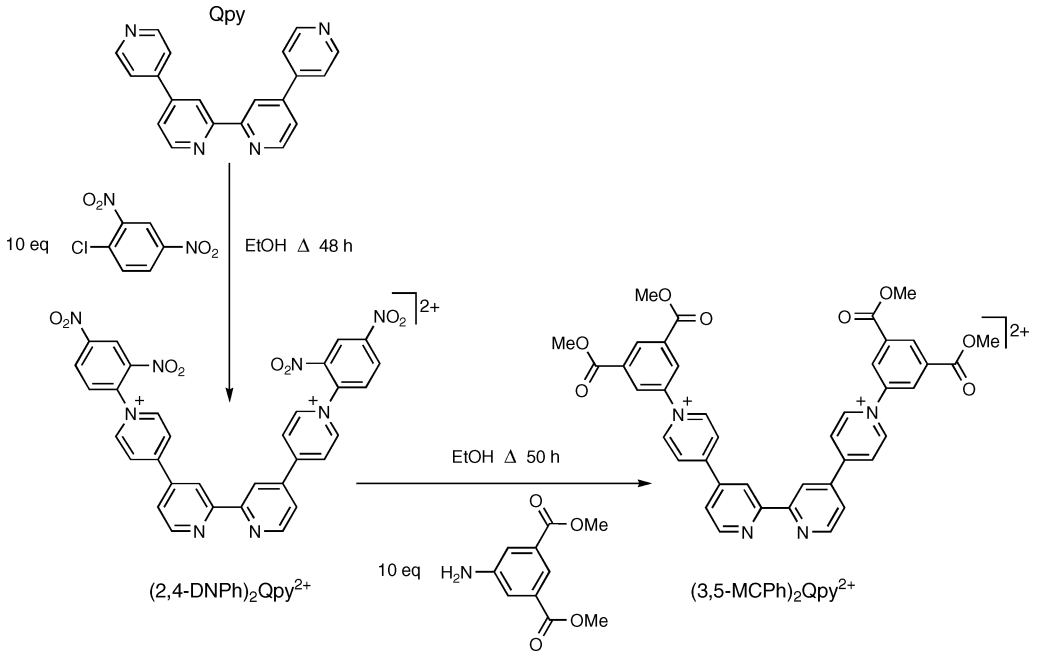

dination chemistry based on *cis*-$Ru^{II}Cl_2(DMSO)_4$[11] in the presence of silver(I) tosylate. The complex salts **5**−**7** (Figure 1) were prepared similarly by using $Fe^{II}(BF_4)_2 \cdot 6H_2O$ as the precursor. Attempts to isolate a pure sample of the compound $[Fe^{II}\{(3,5\text{-MCPh})_2Qpy^{2+}\}_3][PF_6]_8$ were unfortunately unsuccessful.

Electronic Spectroscopy Studies. The UV−visible absorption spectra of salts **1**−**7** have been measured in acetonitrile, and the results are presented in Table 1. These spectra feature intense intraligand $\pi \rightarrow \pi^*$ absorptions in the UV region, together with intense, broad $d(M^{II}) \rightarrow \pi^*(L)$ (M = Ru/Fe, L = N-substituted quaterpyridinium ligand) visible MLCT bands, featuring two maxima in each case. The energy separation between the two MLCT maxima decreases as R changes in the order Me > Ph > 4-AcPh = 3,5-MCPh, and lies in the range of 0.60−0.49 eV for the Ru^{II} complexes and 0.66−0.58 eV for their Fe^{II} analogues. The MLCT bands of the Fe^{II} complexes are somewhat less intense and red-shifted when compared with those of their Ru^{II} counterparts, by ca. 0.4 and 0.3 eV for the lower energy (LE) MLCT and the higher energy (HE) MLCT, respectively. These shifts arise from the higher energies of the metal-based HOMOs in the Fe^{II} complexes due to the increased electron density at the Fe^{II} centers when compared with their Ru^{II} analogues. Representative UV−visible spectra of salts **3** and **5**−**7** are shown in Figure 2.

Within the two series, **1**−**4** and **5**−**7**, the energies of both of the MLCT bands decrease on moving from R = Me to Ph, but subsequent structural modifications to R = 4-AcPh or 3,5-MCPh produce only very slight or negligible further changes in these energies. These red-shifting effects are more pronounced in the HE MLCT bands which shift by ca. 0.1 eV on moving from R = Me to Ph, while the corresponding shifts for the LE MLCT bands are ca. 0.05 eV. It therefore seems likely that the HE MLCT corresponds with a transition from a metal-based HOMO to a π^* MO mainly centered on the pyridinium rings, the energy of which is influenced most strongly by the N-substituent. The LE MLCT can then be ascribed to a transition from a HOMO to a LUMO which is based primarily on the chelating rings and therefore senses changes in R less strongly. The MLCT spectra of **1**−**7** can be compared with those of previously studied 1D[25a] and V-shaped[12,27] Ru^{II} ammine complexes of *N*-R-4,4′-bipyridinium and *N*″,*N*‴-R_2-2,2′:4,4″:4′,4‴-quaterpyridinium

Table 1. UV−Visible Absorption Data for Complex Salts **1**−**7** in Acetonitrile[a]

complex salt	λ_{max}, nm (ϵ, $M^{-1}\,cm^{-1}$)	E_{max} (eV)	assignment
1 $[Ru^{II}(Me_2Qpy^{2+})_3][PF_6]_8$	486 (37300)	2.55	d → π*
	394 (26400)	3.15	d → π*
	324 (55000)	3.83	π → π*
	258 (122500)	4.81	π → π*
2 $[Ru^{II}(Ph_2Qpy^{2+})_3][PF_6]_8$	496 (37300)	2.50	d → π*
	410 (26100)	3.02	d → π*
	328 (65700)	3.78	π → π*
	290 (72100)	3.28	π → π*
	256 (89300)	4.84	π → π*
3 $[Ru^{II}\{(4\text{-AcPh})_2Qpy^{2+}\}_3][PF_6]_8$	498 (49500)	2.49	d → π*
	416 (33500)	2.98	d → π*
	330 (81000)	3.76	π → π*
	290 (116200)	4.28	π → π*
	258 (117700)	4.81	π → π*
4 $[Ru^{II}\{(3,5\text{-MCPh})_2Qpy^{2+}\}_3][PF_6]_8$	498 (53800)	2.49	d → π*
	416 (35200)	2.98	d → π*
	332 (69300)	3.73	π → π*
	270 (125800)	4.59	π → π*
5 $[Fe^{II}(Me_2Qpy^{2+})_3][PF_6]_8$	574 (26000)	2.16	d → π*
	440 (18800)	2.82	d → π*
	330 (44700)	3.76	π → π*
	258 (115800)	4.81	π → π*
6 $[Fe^{II}(Ph_2Qpy^{2+})_3][PF_6]_8$	584 (32500)	2.12	d → π*
	454 (22000)	2.73	d → π*
	294 (103000)	4.22	π → π*
	260 (113700)	4.77	π → π*
7 $[Fe^{II}\{(4\text{-AcPh})_2Qpy^{2+}\}_3][PF_6]_8$	586 (33600)	2.12	d → π*
	460 (22900)	2.70	d → π*
	292 (135500)	4.25	π → π*
	264 (127800)	4.70	π → π*

[a] Solutions ca. $3-8 \times 10^{-5}$ M.

(27) Coe, B. J.; Harris, J. A.; Brunschwig, B. S. *Dalton Trans.* **2003**, 2384−2386.

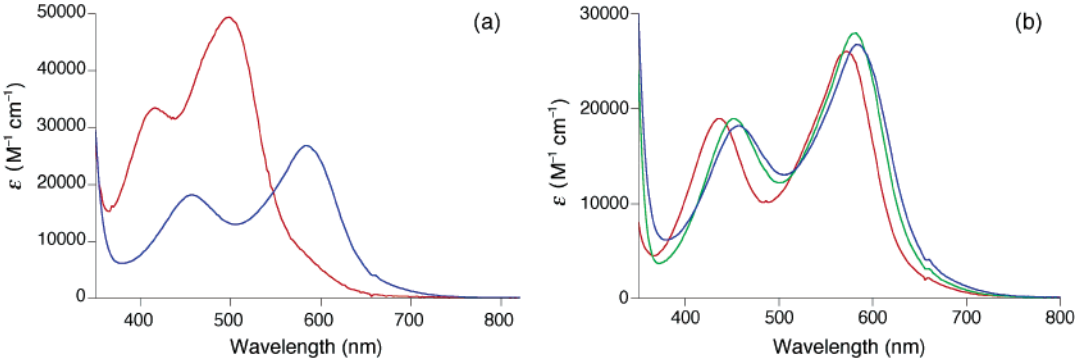

Figure 2. Electronic absorption spectra of (a) **3** (red) and **7** (blue); (b) **5** (red), **6** (green), and **7** (blue) at 295 K in acetonitrile.

Table 2. Electrochemical Data for Complex Salts **1**−**7** in Acetonitrile[a]

complex salt	$E_{1/2}$ or E, V vs Ag–AgCl (ΔE_p, mV)					
	$M^{III/II}$ [b]	$L^{+/0}/L^{2+/0}$ [b]	$L^{0/-}/L^{0/2-}$ [b]	$M^{III/II}$ [c]	$L^{+/0}/L^{2+/0}$ [c]	$L^{0/-}/L^{0/2-}$ [c]
1 $[Ru^{II}(Me_2Qpy^{2+})_3][PF_6]_8$	1.61 (160)[d]	−0.60 (160) −0.74 (160)	−1.28 (290)	1.64 (110)	−0.66 (140)	*g*
2 $[Ru^{II}(Ph_2Qpy^{2+})_3][PF_6]_8$	1.63 (200)[d]	−0.52 (250)	*g*	1.65 (110)	−0.49 (90)	*g*
3 $[Ru^{II}\{(4\text{-}AcPh)_2Qpy^{2+}\}_3][PF_6]_8$	1.74[e]	−0.42[f]	−1.11[f]	1.67 (180)[d]	−0.41[f]	−1.11,[f] −1.30[f]
4 $[Ru^{II}\{(3,5\text{-}MCPh)_2Qpy^{2+}\}_3][PF_6]_8$	*g*	−0.43[f]	−1.10[f]	1.68[e]	−0.40[f]	−1.16,[f] −1.37[f]
5 $[Fe^{II}(Me_2Qpy^{2+})_3][PF_6]_8$	1.38 (250)[d]	−0.69[f]	−0.99[f]	1.43(150)	−0.68,[f] −0.92,[f]	−1.26[f]
6 $[Fe^{II}(Ph_2Qpy^{2+})_3][PF_6]_8$	1.42 (250)[d]	−0.52[f]	−1.11[f]	1.43(180)	−0.47[f]	−1.17[f]
7 $[Fe^{II}\{(4\text{-}AcPh)_2Qpy^{2+}\}_3][PF_6]_8$	1.66[e]	−0.39[f]	−1.08[f]	1.47(230)	−0.39[f]	−1.16,[f] −1.70[f]

[a] Solutions ca. 10^{-3} M in analyte and 0.1 M in $[NBu^n_4]PF_6$ with a scan rate of 200 mV s^{-1}. Ferrocene internal reference $E_{1/2} = 0.47$ V, $\Delta E_p = 90$ mV. [b] Using a Pt disk working electrode. [c] Using a glassy carbon working electrode. [d] Irreversible, $i_{pa} > i_{pc}$. [e] E_{pa} for an irreversible oxidation process. [f] E_{pc} for an irreversible reduction process. [g] Not observed.

ligands. In such complexes, red-shifts of up to 0.15 eV are observed on moving from R = Me to Ph, and further shifts of as much as 0.08 eV occur on moving to R = 4-AcPh.[25a] In all of the complexes studied, the observed red-shifts arising from changes in R can be attributed to the steadily increasing electron deficiency of the pyridinium groups.

Electrochemical Studies. The new complex salts **1**−**7** were studied by cyclic voltammetry in acetonitrile, and the results are presented in Table 2. Despite the fact that the individual redox-active centers in these complexes show well-behaved and often fully reversible redox processes in other related compounds,[12,25,28] the combination of the $[M^{II}(bpy)_3]^{2+}$ (M = Fe, Ru) and *N*-Me/aryl−pyridinium units in **1**−**7** leads to rather poorly defined electrochemical behavior, which unfortunately limits the potential for deriving structure−property correlations. When using a platinum working electrode, all of the complexes show quasi-reversible or irreversible $M^{III/II}$ oxidation waves, together with two or more quasi-reversible and irreversible ligand-based reduction processes. The use of a glassy carbon working electrode gives somewhat improved cyclic voltammograms in which a few of the waves are essentially reversible. Despite the limited quality of the available data, two trends can be identified. First, the $Fe^{III/II}$ waves are found at lower potentials by ca. 200 mV when compared with the $Ru^{III/II}$ waves in analogous complexes, due to the greater electron-richness of the Fe^{II} centers. This difference is predictable and is also reflected in the MLCT data (see above). Second, the ligand-based reductions occur at higher potentials in the complexes of the *N*-aryl ligands as opposed to those of Me_2Qpy^{2+}. This trend is due to the increased electron-accepting ability of the pyridinium groups in the former complexes and is also manifested in the MLCT data (see above) and in previously reported related compounds.[12,25]

Table 3. MLCT Absorption, Luminescence, and HRS Data for Complex Salts **1**−**7** in Acetonitrile

complex salt	λ_{max} (nm)	λ_{em}[a] (nm)	ϵ (M^{-1} cm^{-1})[b]	$\beta_{yyy,800}$[c] (10^{-30} esu)
1 $[Ru^{II}(Me_2Qpy^{2+})_3][PF_6]_8$	486, 394	671	25300	170 ± 21
2 $[Ru^{II}(Ph_2Qpy^{2+})_3][PF_6]_8$	496, 410	685	25300	270 ± 35
3 $[Ru^{II}\{(4\text{-}AcPh)_2Qpy^{2+}\}_3][PF_6]_8$	498, 416	694	30200	281 ± 35
4 $[Ru^{II}\{(3,5\text{-}MCPh)_2Qpy^{2+}\}_3][PF_6]_8$	498, 416	694	31300	290 ± 35
5 $[Fe^{II}(Me_2Qpy^{2+})_3][PF_6]_8$	574, 440	*d*	10600	78 ± 10
6 $[Fe^{II}(Ph_2Qpy^{2+})_3][PF_6]_8$	584, 454	*d*	6900	80 ± 10
7 $[Fe^{II}\{(4\text{-}AcPh)_2Qpy^{2+}\}_3][PF_6]_8$	586, 460	*d*	7800	110 ± 15

[a] Emission maximum. [b] Molar extinction coefficient at 400 nm. [c] First hyperpolarizability measured by using an 800 nm Ti^{3+}:sapphire laser fundamental. The quoted cgs units (esu) can be converted into SI units (C^3 m^3 J^{-2}) by dividing by a factor of 2.693×10^{20}. [d] Not observed.

Hyper-Rayleigh Scattering Studies. The β_{yyy} values of **1**−**7** were measured in acetonitrile solutions by using the HRS technique[14−16] with a 800 nm Ti^{3+}:sapphire laser, and the results are collected in Table 3. Initial experiments using a 1300 nm laser fundamental produced no meaningful results due to overwhelming luminescence from the Ru^{II} complexes around the second harmonic (SH) wavelength of 650 nm and no detectable signals from the nonluminescent Fe^{II} complexes. Such contrasting emission properties are to be expected for such $[M^{II}(bpy)_3]^{2+}$-based (M = Fe, Ru) species.[28] As expected, the lower-energy absorbing complexes in **3** and **4** also have the lowest energy emissions. The long-lived luminescence contributions at 650 nm from the Ru^{II} complexes could be demodulated by using high amplitude modulation frequencies (even at 80 MHz),[16] but in that case, no harmonic scattering signals could be detected. None of **1**−**7** shows any absorption at 800 nm nor

(28) (a) Juris, A.; Balzani, V.; Barigelletti, F.; Campagna, S.; Belser, P.; von Zelewsky, A. *Coord. Chem. Rev.* **1988**, *84*, 85−277. (b) Ferrere, S. *Inorg. Chim. Acta* **2002**, *329*, 79−92.

Table 4. Visible Absorption and Stark Spectroscopic Data for Complex Salts **1**−**7**

complex salt	component	ν_{max}[a] (cm^{-1})	λ_{max}[a] (nm)	E_{max}[a] (eV)	f_{os}	μ_{12}[b] (D)	$\Delta\mu_{12}$ (D)	$\Delta\mu_{ab}$[c] (D)	r_{12}[d] (Å)	r_{ab}[e] (Å)	c_b^{2}[f]	H_{ab}[g] (cm^{-1})	β_0[h] (10^{-30} esu)	$\Sigma\beta_0$ (10^{-30} esu)	N[i]	β_{EN}[j] (10^{-30} esu)
1 $[Ru^{II}(Me_2Qpy^{2+})_3][PF_6]_8$	triplet	17359	576	2.15	0.002	0.5	12.9	12.9	2.7	2.7	0.00	700	1	68	72	11.1
	MLCT-1	20149	496	2.50	0.17	4.2	7.9	11.6	1.6	2.4	0.16	7400	26			
	MLCT-3	25240	396	3.13	0.39	5.8	10.3	15.5	2.2	3.2	0.17	9400	41			
2 $[Ru^{II}(Ph_2Qpy^{2+})_3][PF_6]_8$	triplet	16988	589	2.11	0.02	1.4	7.0	7.5	1.5	1.6	0.04	3200	4	114	108	10.2
	MLCT-1	19901	502	2.47	0.16	4.2	10.0	13.1	2.1	2.7	0.12	6400	34			
	MLCT-3	24553	407	3.04	0.51	6.7	13.5	19.0	2.8	4.0	0.14	8600	76			
3 $[Ru^{II}\{(4\text{-}AcPh)_2Qpy^{2+}\}_3][PF_6]_8$	triplet	16843	594	2.09	0.02	1.4	7.3	7.8	1.5	1.6	0.03	3100	4	79	120	6.0
	MLCT-1	19752	506	2.45	0.13	3.7	11.5	13.7	2.4	2.9	0.08	5400	31			
	MLCT-3	24062	416	2.98	0.30	5.1	12.8	16.4	2.7	3.4	0.11	7500	44			
4 $[Ru^{II}\{(3,5\text{-}MCPh)_2Qpy^{2+}\}_3][PF_6]_8$	triplet	16864	593	2.09	0.02	1.7	7.7	8.4	1.6	1.8	0.04	3400	6	97	132	6.4
	MLCT-1	19736	507	2.45	0.15	4.0	11.1	13.7	2.3	2.9	0.10	5800	35			
	MLCT-3	24128	414	2.99	0.35	5.5	14.1	17.9	2.9	3.7	0.11	7400	56			
5 $[Fe^{II}(Me_2Qpy^{2+})_3][PF_6]_8$	MLCT-1	17225	581	2.14	0.16	4.4	6.1	10.6	1.3	2.2	0.22	7100	30	86	72	14.1
	MLCT-3	22531	444	2.79	0.35	5.8	11.2	16.1	2.3	3.4	0.15	8100	56			
6 $[Fe^{II}(Ph_2Qpy^{2+})_3][PF_6]_8$	MLCT-1	16950	590	2.10	0.16	4.5	7.4	11.6	1.5	2.4	0.18	6500	39	121	108	10.8
	MLCT-3	21675	461	2.69	0.37	6.1	13.9	18.4	2.9	3.8	0.12	7100	82			
7 $[Fe^{II}\{(4\text{-}AcPh)_2Qpy^{2+}\}_3][PF_6]_8$	MLCT-1	16788	596	2.08	0.14	4.3	7.9	11.6	1.6	2.4	0.16	6200	39	151	120	11.5
	MLCT-3	21324	469	2.64	0.41	6.4	16.4	20.8	3.4	4.3	0.11	6500	112			

[a] Maxima for Gaussian functions used to fit to spectral data recorded in a butyronitrile glass at 77 K. [b] Calculated using eq 3; f_{os} obtained from $(4.32 \times 10^{-9}$ M $cm^2)A$, where A is the area under the absorption peak. [c] Calculated from eq 2. [d] Calculated from $\Delta\mu_{12}/e$. [e] Effective (localized) electron-transfer distance calculated from $\Delta\mu_{ab}/e$. [f] Calculated from eq 4. [g] Calculated from eq 5. [h] Calculated from eq 6. [i] The total number of π-bonding electrons in the complex cation. [j] Electron-normalized off-resonant first hyperpolarizability, defined as $\Sigma\beta_0/N^{3/2}$ (see ref 35).

emission at the SH wavelength of 400 nm, but all of these compounds do show absorption at 400 nm, especially the Ru^{II} complexes (Figure 2). The retrieved β_{yyy} values at 800 nm are hence strongly resonance enhanced.

For the Ru^{II} complexes, the extent of absorption at 400 nm is the same for **1** and **2** and somewhat larger for **3** and **4**. Therefore, the observed, relatively substantial increase in β on moving from **1** to its *N*-aryl counterparts may be attributable mostly to the presence of more strongly electron-accepting pyridinium groups, as observed previously in 1D[25a] and V-shaped[12,27] Ru^{II} ammine complexes of related ligands. A corresponding trend is observed rather less convincingly with the Fe^{II} complexes in **5**−**7**, and this may be because resonance due to the HE MLCT band is stronger in **5** when compared to that of **7** and **8**. At first glance, these HRS data clearly indicate that the Ru^{II} complexes have larger β values when compared with those of their Fe^{II} counterparts. However, this apparent trend is most likely attributable to the much more pronounced effects of resonance enhancement in **1**−**4**. Although the MLCT and electrochemical data (above) clearly show that the Fe^{II} centers have stronger electron-donating abilities than their Ru^{II} counterparts, the intensities of the MLCT bands, and hence their transition dipole moments, are somewhat lower for the Fe^{II} compounds. Because β values generally increase with decreasing ICT energy and increasing intensity, it is therefore not easy to predict whether the Ru^{II} or the Fe^{II} complexes will have the largest NLO responses. Previous comparative studies involving analogous dipolar Ru^{II} and Fe^{II} complexes in which MLCT transitions dominate the NLO responses have generally concluded that the Fe^{II} species possess the largest β values.[4g,29] However, some exceptions to this trend have been reported recently.[30]

Stark Spectroscopic Studies. To further probe their molecular NLO responses and related properties, **1**−**7** were studied by electronic Stark effect (electroabsorption) spectroscopy in butyronitrile glasses at 77 K, and the results are presented in Table 4.

Previous studies on $[Ru^{II}(bpy)_3]^{2+}$ have given a $\Delta\mu_{12}$ value of 6.8 D, although contributions from overlapping bands were neglected.[31] In our systems, the use of Gaussian fitting has made it possible to determine values of $\Delta\mu_{12}$ for multiple MLCT bands. The absorption spectra were fit by using three or four Gaussian curves, the first and second derivatives of which were used to fit the Stark spectra. Representative absorption and Stark spectra, including all fits for **3** and **7**, are presented in Figure 3. The main features of the absorption spectra can be fit with three Gaussian curves, but in the case of **1**−**4**, a very low intensity Gaussian curve was placed to low energy in order to fit the Stark signal due to a spin-forbidden transition to a triplet excited state.[32] This transition is visible in the absorption spectra as a shoulder to low energy of the more intense singlet LE MLCT band and grows in intensity upon ligand *N*-arylation. Of the three Gaussian curves used to fit the transitions to singlet excited states (MLCT-1, MLCT-2, and MLCT-3, respectively), only two, MLCT-1 and MLCT-3, contribute significantly to the observed Stark signal.

The absence of any significant Stark effect associated with the Gaussian curves labeled MLCT-2 indicates that the excited states populated by the corresponding transitions are not highly dipolar. However, the excited states populated by MLCT-1 and MLCT-3 are dipolar, as evidenced by the observation of significant Stark signals. Since the ground states of complexes of the form $[M^{II}(L-L)_3]^{n+}$ (M = Ru, etc.; L−L = symmetrical diimine ligand; n = 2 or 3) are octupolar, the observation of Stark signals indicates the presence of localized excited states, the associated $\Delta\mu_{12}$ values of which are determined directly by the Stark measurements.[33]

(29) (a) Calabrese, J. C.; Cheng, L.-T.; Green, J. C.; Marder, S. R.; Tam, W. *J. Am. Chem. Soc.* **1991**, *113*, 7227−7232. (b) Wenseleers, W.; Gerbrandij, A. W.; Goovaerts, E.; Garcia, M. H.; Robalo, M. P.; Mendes, P. J.; Rodrigues, J. C.; Dias, A. R. *J. Mater. Chem.* **1998**, *8*, 925−930. (c) Garcia, M. H. et al. *Organometallics* **2002**, *21*, 2107−2118. (d) Garcia, M. H. et al. *Eur. J. Inorg. Chem.* **2003**, 3895−3904.
(30) Powell, C. E. et al. *Inorg. Chim. Acta* **2003**, *352*, 9−18.
(31) Oh, D. H.; Boxer, S. G. *J. Am. Chem. Soc.* **1989**, *111*, 1130−1131.
(32) Kober, E. M.; Meyer, T. J. *Inorg. Chem.* **1982**, *21*, 3967−3977.
(33) Karki, L.; Hupp, J. T. *Inorg. Chem.* **1997**, *36*, 3318−3321.

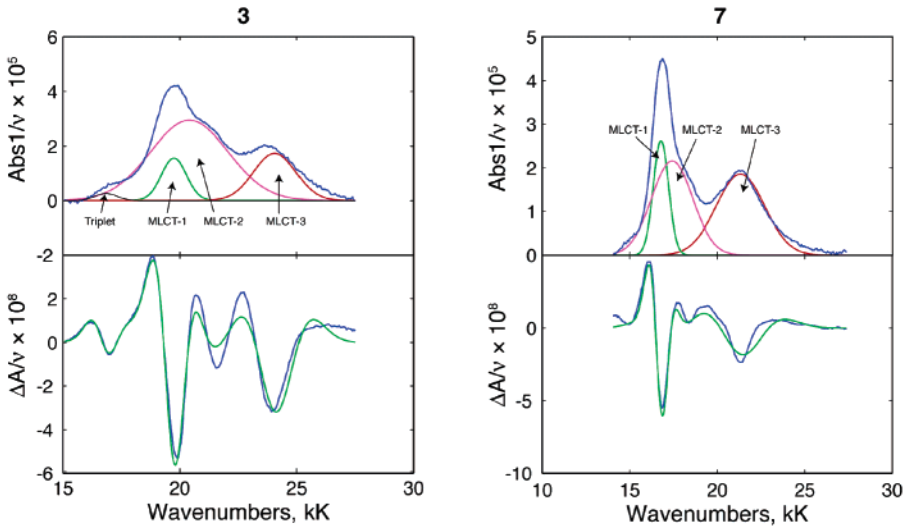

Figure 3. Stark spectra and calculated fits for **3** and **7** in external electric fields of 3.32 and 2.93 × 10^7 V $m^{-1,}$ respectively. Top panel: absorption spectrum illustrating Gaussian curves utilized in data fitting. Bottom panel: electroabsorption spectrum, experimental (blue) and fits (green) according to eq 1.

The E_{max} values for the spin-forbidden excitations to the triplet MLCT state for **1**−**4** are ca. 0.35 eV lower in energy than that of MLCT-1 and red-shift slightly with increasing ligand acceptor strength. These shifts are similar in magnitude to those of MLCT-1, indicating that the excitations are to the triplet excited states corresponding to the singlet excited states populated by the MLCT-1 transitions. However, the values of $\Delta\mu_{12}$ for these spectroscopically forbidden excitations differ from those derived for either MLCT-1 or MLCT-3. This discrepancy can be explained by the relatively large uncertainties associated with the triplet data due to the low intensities and consequent high signal-to-noise of the absorption bands.

The measured μ_{12} values lie in the range of 3.7−4.5 D for MLCT-1 and 5.1−6.7 D for MLCT-3. In all cases, μ_{12} for MLCT-3 is larger than that for MLCT-1, but there is no apparent trend with changing the ligand N-substituent or metal center. Similarly, the $\Delta\mu_{12}$ values for MLCT-3 are larger than those for MLCT-1. The magnitude of the difference is larger in complexes **5**−**7**, where $\Delta\mu_{12}$ for MLCT-3 is ca. double that for MLCT-1. The $\Delta\mu_{12}$ values for MLCT-1 are comparable with reported values for $[Ru^{II}(bpy)_3]^{2+}$, the spectrum of which is dominated by a low energy band with no other significant bands contributing to the Stark spectrum.[31] In both series, **1**−**4** and **5**−**7**, the $\Delta\mu_{12}$ values for both MLCT-1 and MLCT-3 increase upon *N*-arylation, but there is no apparent trend on changing the metal center.

As noted in the previous discussion of the visible absorption spectra (above), the greater sensitivity of the HE MLCT (denoted MLCT-3) to increasing ligand acceptor strength suggests that the LUMO associated with this transition lies further out toward the pyridinium ring, when compared with the LUMO involved in the LE MLCT process. The corresponding delocalized electron-transfer distances r_{12} are consistent with this hypothesis, showing that the electron-transfer distances for MLCT-3 are larger than those for MLCT-1 by ca. 13−37%. The r_{12} values for MLCT-1 are smaller in every case for **5**−**7** when compared with those of **1**−**4**, indicating that the LUMO for MLCT-1 lies closer to the metal center in the Fe^{II} complexes.

The H_{ab} values for MLCT-1 and MLCT-3 lie in the ranges of 7400−5400 and 9400−6500 cm^{-1}, respectively, and decrease on *N*-arylation. The corresponding values of c_b^2 range from 0.22 to 0.08 and 0.17 to 0.11 and also decrease on *N*-arylation. In **1**−**4**, the c_b^2 values for MLCT-3 are larger than those for MLCT-1, but in **5**−**7**, this trend is reversed. The magnitudes of H_{ab} and c_b^2 are consistent with the assignment of the visible absorptions as arising from MLCT transitions in which the degree of delocalization is limited.

Given that dipolar excited states are involved, it is not unreasonable to apply the standard two-state model[34] to estimate static first hyperpolarizabilities from the Stark data for **1**−**7**. The values of β_0 calculated by using eq 6 are larger for MLCT-3 than for MLCT-1 because the lower energy of MLCT-1 is more than offset by the larger values of μ_{12} and $\Delta\mu_{12}$ for MLCT-3. In general, there appears to be an increase in β_0 on *N*-arylation, and the values for complexes **5**−**7** are comparable to or larger than those of the corresponding Ru^{II} complexes (although note that the estimated experimental errors are ±20%). The latter result is largely attributable to the lower charge-transfer energies since μ_{12} and $\Delta\mu_{12}$ are similar in magnitude for the two groups of complexes. The β_0 values associated with the triplet MLCT excitations have also been calculated for the sake of completeness. As expected, these values are very small, and do not contribute significantly to the total first hyperpolarizability of the complexes. These Stark-derived β_0 values give perhaps a more accurate description of the NLO responses than the HRS-derived β_{800} values due to the pronounced resonance enhancement in the latter data. Furthermore, the Stark results are in agreement with previous studies comparing analogous Ru^{II} and Fe^{II} complexes, which show that the Fe^{II} complexes have the larger β values.[4g,29]

Recent studies with purely organic dipolar NLO chromophores have included electron-normalized off-resonant first hyperpolarizabilities β_{EN},[35] which are derived by considering the number of π-bonding electrons. Such values are also included in Table 4. Although these β_{EN} data should be treated as quite approximate and the validity of applying such an

(34) (a) Oudar, J. L.; Chemla, D. S. *J. Chem. Phys.* **1977**, *66*, 2664−2668. (b) Oudar, J. L. *J. Chem. Phys.* **1977**, *67*, 446−457.
(35) (a) Kuzyk, M. G. *Phys. Rev. Lett.* **2000**, *85*, 1218−1221. (b) Tripathy, K.; Pérez Moreno, J.; Kuzyk, M. G.; Coe, B. J.; Clays, K.; Myers Kelley, A. *J. Chem. Phys.* **2004**, *121*, 7932−7945.

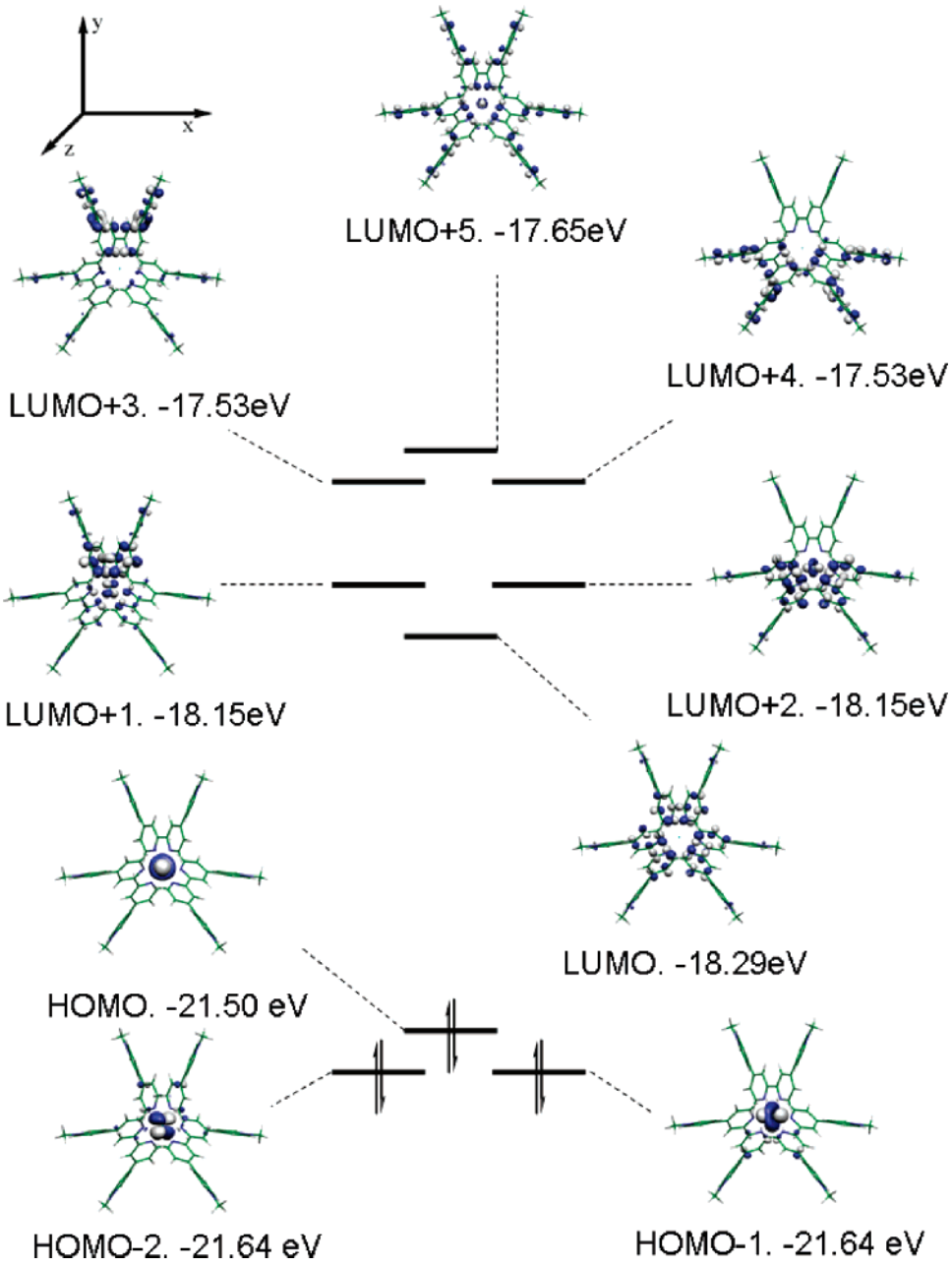

Figure 4. Molecular orbital diagram of the cation in **1** showing the 0.04 contour plots of molecular orbitals calculated by B3P86/LanL2DZ.

approach to metal-containing octupolar chromophores has not been established, the results indicate that β_{EN} actually *decreases* on replacing an *N*-Me with an *N*-aryl substituent. However, increases in the NLO responses on moving from the Ru^{II} complexes to their Fe^{II} analogues are still apparent.

Theoretical Studies. To shed further light on the molecular electronic structures of **1**−**7**, we have performed theoretical calculations on the representative model complex chromophores in salts **1** and **5** by using Gaussian 03. The geometries were optimized at the B3P86/LanL2DZ model chemistry, restricted to D_3 symmetry, and both finite field (FF) and TD-DFT calculations used the same level of theory.

The standard orientation of the molecule places the *z* axis aligned to the C_3 axis and the *y* axis aligned to one of the C_2 axes. The zero frequency first hyperpolarizabilities calculated by using the FF method are $\beta_{yyy} = -\beta_{yxx} = 25.3 \times 10^{-30}$ esu for the cation in **1** and $\beta_{yyy} = -\beta_{yxx} = 11.4 \times 10^{-30}$ esu for the cation in **5** (with β defined according to the perturbation series convention).[20] The observation of such a relationship between the two tensor components β_{yyy} and β_{yxx} is consistent with **1** and **5** being octupolar molecules that have zero ground-state dipole moment (although note that here the *x* and *y* axes are interchanged when compared with previous studies).[2b] The decrease in the molecular hyperpolarizability on moving from Ru^{II} to Fe^{II} complex parallels the experimental HRS trends, and the large differences between the theoretical and HRS values are attributable to the previously mentioned resonance enhancement of the experimental data, and possibly also solvation effects. The analysis of DFT molecular orbitals reveals that the HOMOs are mainly derived from metal d orbitals, while the LUMOs are ligand π orbitals (Figures 4 and 5). It is worth noting the existence of pairs of degenerate orbitals which do not display trigonal symmetry and can therefore give rise to localized excited states.[36]

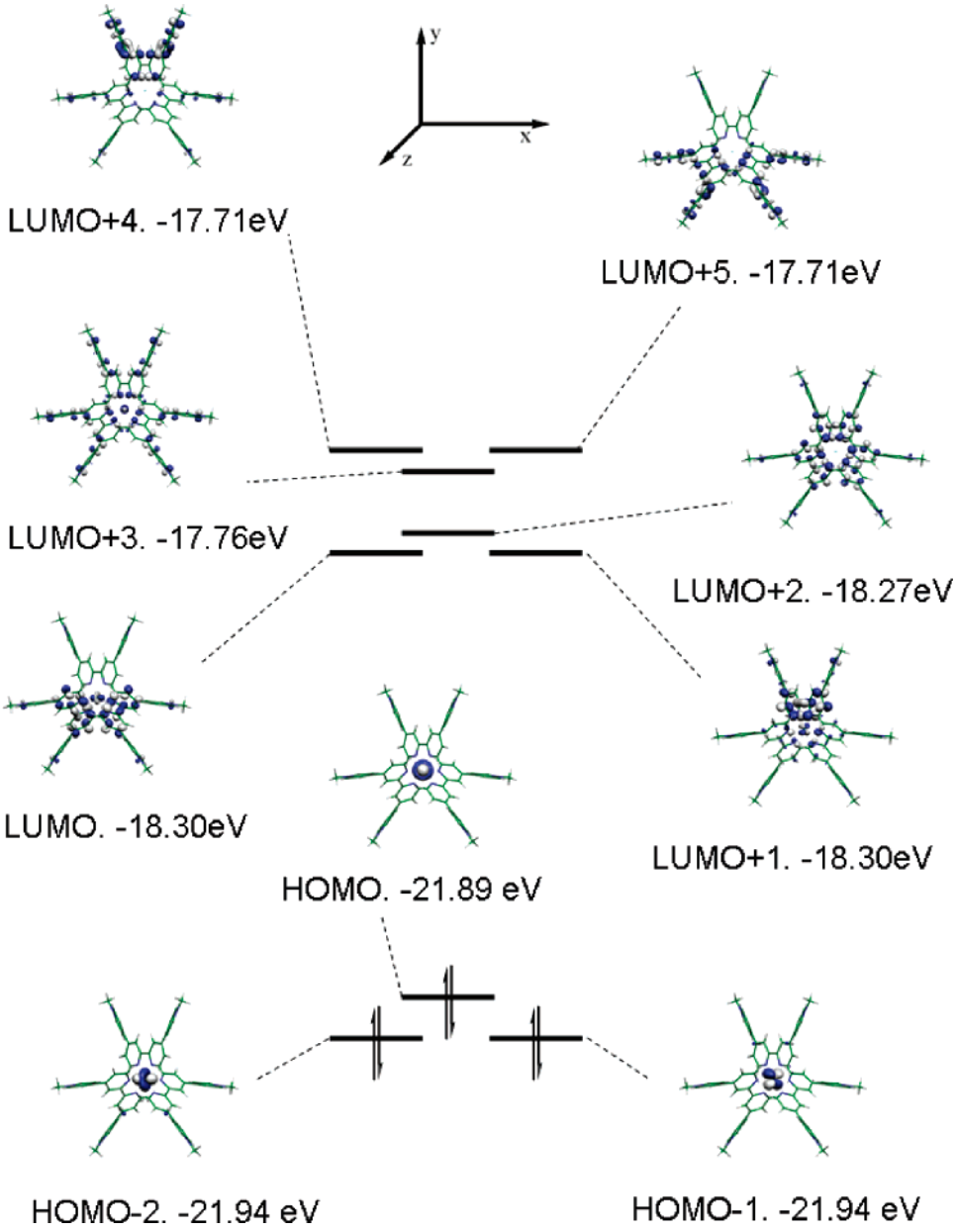

Figure 5. Molecular orbital diagram of the cation in **5** showing the 0.04 contour plots of molecular orbitals calculated by B3P86/LanL2DZ.

The existence of excited states with nonzero dipole moment has been explored by using TD-DFT calculations, and the results are shown in Table 5. It can be seen that for the cation in salt **1** there is a reasonably good degree of agreement between the theoretical and experimental data (Tables 1 and 4). Note, however, that the Stark measurements afford only the magnitude, and not the sign, of dipole moment changes. Comparing E_{max}, μ_{12}, and $\Delta\mu_{12}$ values, the electronic transitions calculated at 2.78 eV can be assigned to MLCT-1 observed at 2.50 eV (butyronitrile glass) or 2.55 eV (acetonitrile solution) and the transitions calculated at 3.26 eV to MLCT-3 (3.13 eV in butyronitrile glass and 3.15 eV in acetonitrile solution). It should be noted that the theoretical calculations are performed in the gas phase, and these electronic transitions are expected to display bathochromic shifts in polar solvents (positive solvatochromism). Calculations on the cation in **5** lead to an analogous picture to that described for the cation in **1**, with pairs of degenerate orbitals giving rise to degenerate excited states with nonzero dipole moment (Table 5). However, in contrast with the experimental results, the calculated transition energies for the cation in **5** are blue-shifted when compared to those of the cation in **1**, and consequently, the calculated gas-phase excitation energies are, in this case, well above the experimental values. Assuming that the cation in **5** behaves in a similar way to the cation in **1**, and considering that TD-DFT can give rise to large errors in modeling charge-transfer excitations[37] and that solvent effects have not been included in the calculations, the transitions calculated at 2.91 eV can be assigned to MLCT-1 and those calculated at 3.57 eV can be assigned to MLCT-3.

(36) (a) Lee, Y. K.; Jeon, S. J.; Cho, M. *J. Am. Chem. Soc.* **1998**, *120*, 10921−10927. (b) Cho, M.; Kim, H. S.; Jeon, S. J. *J. Chem. Phys.* **1998**, *108*, 7114−7120. (c) Andraud, C.; Zabulon, T.; Collet, A.; Zyss, J. *Chem. Phys.* **1999**, *245*, 243−261.

(37) (a) Tozer, D. J.; Amos, R. D.; Handy, N. C.; Roos, B. O.; Serrano-Andres, L. *Mol. Phys.* **1999**, *97*, 859−868. (b) Dreuw, A.; Head-Gordon, M. *J. Am Chem. Soc.* **2004**, *126*, 4007−4016.

Table 5. Results of TD-B3P86/LanL2DZ Calculations on the Complex Cations in Salts **1** and **5**[a]

parent salt	E_{max} (eV)	f_{os}	major contributions[b]	polarization	μ_{12} (D)	$\Delta\mu_{12}$ (D)
1	2.63	0.03	H−1 → L (83%) H−2 → L+2 (7%) H−1 → L+1 (7%)	*x*	1.8	−6.5
	2.63	0.03	H−2 → L (83%) H−2 → L+1 (7%) H−1 → L+2 (7%)	*y*	1.8	+6.5
	2.78	0.26	H−1 → L+1 (40%) H−2 → L+2 (40%) H−1 → L (12%)	*x*	5.0	+4.5
	2.78	0.26	H−2 → L+1 (40%) H−1 → L+2 (40%) H−2 → L (12%)	*y*	5.0	−4.5
	3.26	0.11	H → L+4 (93%)	*x*	2.9	+10.6
	3.26	0.11	H → L+3 (93%)	*y*	2.9	−10.6
	3.39	0.16	H−2 → L+5 (90%)	*x*	3.5	+4.3
	3.39	0.16	H−1 → L+5 (90%)	*y*	3.5	−4.3
5	2.77	0.07	H−2 → L+1 (42%) H−1 → L (42%) H → L+1 (5%)	*x*	2.6	−2.4
	2.77	0.07	H−1 → L+1 (42%) H−2 → L (42%) H → L (5%)	*y*	2.6	+2.4
	2.91	0.12	H−2 → L+2 (93%)	*x*	3.2	+1.3
	2.91	0.12	H−1 → L+2 (93%)	*y*	3.2	−1.3
	3.54	0.03	H−1 → L+3 (78%)	*x*	1.5	−2.2
	3.54	0.03	H−2 → L+3 (78%)	*y*	1.5	+2.2
	3.57	0.11	H → L+5 (91%)	*x*	2.9	+9.8
	3.57	0.11	H → L+4 (91%)	*y*	2.9	−9.8

[a] Only transitions with $f_{os} > 0.02$ are included. [b] H = HOMO, L = LUMO; only contributions above 5% are included.

According to our TD-DFT results, there are several pairs of degenerate excited states with nonzero dipole moments that are responsible for the dipolar contribution to the molecular first hyperpolarizability.[38] The transition from the ground state to each of the degenerate excited states in one of these pairs is polarized along a different axis (*y* or *x*), and therefore, the transition to each excited state contributes to a different component of β (β_{yyy} or β_{yxx}, respectively). Furthermore, the degenerate excited states display identical dipole moments, but with opposite signs, and it is therefore expected that the dipolar contribution to β_{yyy} will be identical to minus the contribution to β_{yxx}, as already calculated by using the FF method for the overall hyperpolarizabilities.

It should also be noted that different electronic transitions having the same polarization may have an opposed contribution to the hyperpolarizability due to the different sign of their associated dipole moment change. For instance, in the cation in **1**, the dipole moment change associated with the 2.63 eV transition polarized along the *y* axis (+6.5 D) is opposed to those associated with the *y*-polarized 2.78, 3.26, and 3.39 transitions (−4.5, −10.6, and −4.3 D, respectively), and the same applies to the *x*-polarized transitions. This fact resembles the behavior of other $[Ru^{II}(bpy)_3]^{2+}$ derivatives for which it has been suggested that the contribution of the MLCT transitions is opposed to that of the ILCT transitions[10] and could explain, at least partially, the apparent discrepancies between Stark and HRS experiments since the former determines the dipolar contribution to the hyperpolarizability of each electronic transition, whereas the latter samples the overall hyperpolarizability. However, for the cations in salts **1** and **5**, the contribution of MLCT-1 and MLCT-3 to the hyperpolarizability is additive.

The observation that the quadratic NLO responses of our new, putatively octupolar complex chromophores are primarily associated with electronic transitions to dipolar (as opposed to octupolar) excited states is partially reminiscent of previous results with a donor-substituted $[Ru^{II}(bpy)_3]^{2+}$ derivative,[10] but with the key difference that in the present chromophores the important transitions have MLCT character. Having said this, it is worth noting that the contribution of octupolar excited states in the present chromophores cannot be categorically ruled out. The calculation of octupolar contributions requires transition dipole moments between excited states, quantities which are not accessible via the TD-DFT modeling approach. Indeed, the presence of the Gaussian curves labeled MLCT-2, for which no significant Stark effect is observed (see above), may be relevant in this regard and, therefore, worthy of further investigation. Recent studies have used the ZINDO/SOS approach to derive β values for purely organic octupolar chromophores,[2l] and Claessens et al. have described a combined theoretical/experimental investigation into the effects of structural modification on the relative importance of dipolar and octupolar contributions to the NLO response in subphthalocyanines.[2m,39]

In agreement with the Stark results, TD-DFT predicts a larger $\Delta\mu_{12}$ for the MLCT-3 transition than for MLCT-1 since the latter involves unoccupied orbitals that are mainly located on the pyridyl rings directly coordinated to the metal ion, while the unoccupied orbitals involved in MLCT-3 also have an important contribution from the external pyridinium rings (Figures 4 and 5). The topology of these unoccupied acceptor orbitals also explains the effect of changing from R = Me to aryl in causing a larger bathochromic shift for MLCT-3 than for MLCT-1 (see above).

Conclusions

We have synthesized and characterized the first family of charged 3D, nominally octupolar NLO chromophores in which the β responses are associated only with MLCT (as opposed to intraligand) transitions. HRS measurements at 800 nm show that the Ru^{II} complexes have larger, albeit resonantly enhanced, first hyperpolarizabilities when compared with their Fe^{II} analogues. Stark spectroscopic studies confirm the existence of dipolar excited states and show that the NLO responses have two substantial components, with larger β_0 values for the Fe^{II} complexes. In contrast, the zero frequency first hyperpolarizabilities calculated by using the FF method are $\beta_{yyy} = -\beta_{yxx} = 25.3 \times 10^{-30}$ esu for the Ru^{II} cation in salt **1** and $\beta_{yyy} = -\beta_{yxx}$

(38) It is worth noting here that some of the earlier papers on octupolar molecules (see for example ref 2b) invoke degenerate excited states having zero dipole moment and rationalize the β response by using a three-state model involving the transition dipole moment between excited states as well as that between the ground state and excited states. However, some subsequent papers propose localized degenerate excited states (see for examples ref 36) in such a way that the quadratic NLO response arises from two-state terms involving excited states with nonzero dipole moment (that we refer to here as "dipolar contributions"), as well as three-state terms that do not depend on the excited-state dipole moments but on the transition dipole moments (referred to here as "octupolar contributions").

(39) Note, however, that there is potential for some confusion over terminology here. The term "dipolar contributions" is applied in ref 2m to cone-shaped molecules that display a nonzero ground-state dipole moment due to their lack of planarity. In contrast, the molecules we report have no ground-state dipole moment, and thus the precise meaning of "dipolar contributions" in this context differs from that used by Claessens et al. Because the β responses in **1** and **5** are associated with dipole moment changes on passing from ground to excited states, their origins are thus analogous to those in molecules having a dipolar ground state.

$= 11.4 \times 10^{-30}$ esu for the Fe^{II} cation in salt **5**. The orbital structures of these representative complex cations have been elucidated by using TD-DFT, which reveals pairs of orthogonally (*x*,*y*)-polarized degenerate transitions in both cases, but better agreement between the theoretical and experimental data for the Ru^{II} complex. The most intense low-energy MLCT transition involves LUMOs that are mainly located on the pyridyl rings directly coordinated to the metal ion, while the LUMOs involved in the next lowest-energy MLCT transition also have an important contribution from the external pyridinium rings. These results concur with the experimental observation that the higher-energy MLCT band shows a greater sensitivity to changes in the pyridinium N-substituent. One final point which is perhaps worth noting is that the especially broad visible absorption profiles of our new complex chromophores may render suitably functionalized derivatives of interest for applications in dye-sensitized solar cells.[40] Further studies on these novel chromophores will include the maximization of β responses by modifications of the ligand structures.

Acknowledgment. We thank the EPSRC for support (Grant GR/M93864), and also the Fund for Scientific Research-Flanders (FWO-V, G.0297.04), the University of Leuven (GOA/2000/3), the Belgian Government (IUAP P5/3), MCyT-FEDER (BQU2002-00219), and Gobierno de Aragon-Fondo Social Europeo (E39).

Supporting Information Available: Cartesian coordinates of theoretically optimized geometries for the cations in **1** and **5**; complete refs 4e, 4k, 21, 29c, 29d, and 30 (PDF). This material is available free of charge via the Internet at http://pubs.acs.org.

JA053879X

(40) (a) Coe, B. J.; Curati, N. R. M. *Comments Inorg. Chem.* **2004**, *25*, 147−184. (b) Klein, C.; Nazeeruddin, Md. K.; Liska, P.; Di Censo, D.; Hirata, N.; Palomares, E.; Durrant, J. R.; Grätzel, M. *Inorg. Chem.* **2005**, *44*, 178−180 and references therein.